# *University of Minnesota Solar Vehicle Project*

## *Borealis 3*
## *Structural Report*

## *March 1st, 2005*

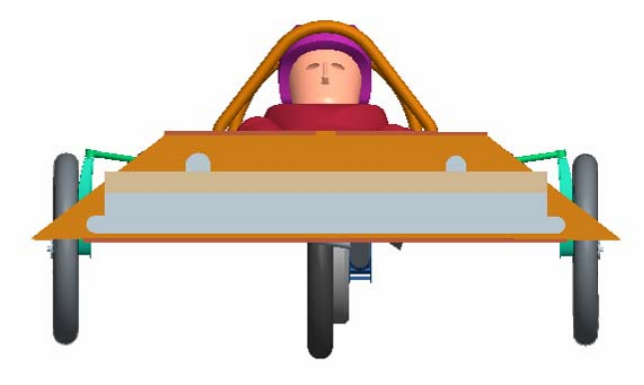

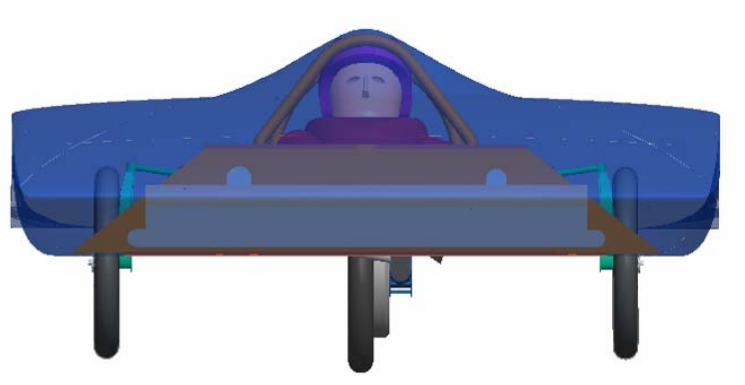

## *Student Contributions*

**Mitch Horn-Wyffels**
**Horn0190@umn.edu**
***Mechanical Team Leader***
**Al Majkrzak**
**Majk0006@umn.edu**
***Mechanical Team Leader***

**Will Blee**
**Josh Malmquist**
**Peter Meinz**
**Erik Anderson**
**Ben Thompson**
**John Wanner**
**Aaron Westman**

## *Faculty Advisor*

**Dr. Patrick J. Starr**
**pjstarr@me.umn.edu**
**Professor of Mechanical Engineering**
**University of Minnesota**


**Figure 1: Borealis 3 Mechanical Team with Borealis II at FSGP 2004**

**Left to Right:** Travis Lee, Ellie Field, Brett Portner-Kuhlow, Al Majkrzak, Mitch Horn-Wyffels, Erik Anderson, Carl Bienert, Peter Meinz, Will Blee, and Jason Halpern.

**Not Pictured:** Jacques Dolan, Josh Malmquist, Andy Sherman, Matthew Stignani, Ben Thompson, and John Wanner.

# Introduction

Since 1990 the University of Minnesota Solar Vehicle Project (UMNSVP) has produced six world class race vehicles. For the 2005 North American Solar Challenge (NASC) and Formula Sun Grand Prix (FSGP) events the UMNSVP will enter Borealis 3, its seventh solar vehicle.

Borealis 3 builds upon the lessons learned through the team's previous six designs. It is the third in the Borealis series of vehicles which have brought the team much success. Major improvements for Borealis 3 include a 10% reduction in vehicle weight, improved strength and conductive properties of our top shell, much improved aerodynamics, and an attention to detail and craftsmanship above and beyond all of our previous vehicles.

It is the intent of this paper to document the engineering decisions and features included in Borealis 3. In addition, this report will demonstrate to the NASC race officials that our entry is a safe, road worthy, and competitive vehicle. Any questions or concerns regarding the content of this report may be addressed to either of our mechanical team leaders or our faculty advisor.

Allen A. Majkrzak
Borealis 3 Mechanical Team Leader

# Table of Contents



# Mechanical Systems Analysis

### Loading Conditions for All Analyses

Figure 26 shows the forces on the bottom of the tires for the following conditions. The total vehicle weight is W (assumed to be 560 [lbm]) and the center of gravity is at one third of the wheelbase behind the front axle. We expect to achieve this value within one inch, so it is assumed for the analysis.

-The static load on each wheel is 1 [G] or 1/3 W.
-The bump load is 4 [G] or 4/3 W.
-The brake load is 1 [G] and assumed at the front wheels only so each front wheel braking load is 1/2 W.
-The cornering load is shown for a right hand turn and assumes a 1[G] lateral acceleration and incipient tipping, with the “outside” front wheel providing lateral force 2/3 W, the “inside” front wheel providing no lateral force, and the rear wheel providing 1/3 W.
-The drive and braking forces at the rear wheel are relatively small and produce small chassis loads compared to the bump and cornering, and so are ignored.

These load cases are similar to those used in the GM Sunraycer Case History, Lecture 6-1: Structure (Chassis) by Ray Morgan and Herman Drees, and have proven successful on all the University of Minnesota solar vehicles since 1993.

### Mounting to Composite Paneling

Two part aluminum inserts are used at all locations that require fastening to the composite panels. The aluminum inserts are tested by the manufacturer to 1500 [lbf] for in-plane shear and are used for all attached components under load. The design of the insert is intended to handle bolt clamping load while distributing axial and shear loads to the sandwich panels. These inserts were used successfully on all previous U of M solar vehicles.

## *Front Suspension*

### Material Specifications

The front suspension system is a double A-arm design optimized for low weight and low tire scrub. The lower a-arms are made from 0.750 [in] OD by 0.058 [in] wall 4130 steel tubing. The upper a-arms are made from 0.625 [in] OD by 0.058 [in] wall 4130 steel tubing. The wheel hubs and uprights are CNC machined from 7075-T6 aluminum. The axles are made from solid 0.669 [in] OD heat-treated 4140 steel.

The lower a-arm uses a 0.375 [in] bore spherical bearing at the lower upright joint and is mounted to the chassis with 0.250 [in] bore high angle rod ends with 0.375 [in] shanks. The lower a-arm brackets are machined from 6061-T6 aluminum and each attaches to two chassis panels. Sharing the load across two panels spreads the load and reinforces the panel joint. The top a-arm uses a 0.375 [in] bore spherical bearing at the top upright joint and is mounted with 0.313 [in] bore rod ends with 0.313 [in] shanks. The top a-arm is attached to the chassis with sandwiched 0.125 [in] sheet 6061-T6 aluminum brackets. These brackets bolt into the chassis via vertical carbon fiber panels. The panels are loaded in plane with their skins. This is the preferred method of loading with this type of composite paneling. The panels are aligned with the a-arm legs so that the loads are in the plane of each panel. The a-arms are designed so that no rod ends are in bending under any load condition. This allows each arm to be treated as a two-force member. The assembled layout of the front suspension is shown in figure 2.

All hardware used in the front suspension is AN-aircraft or MS-military spec grade bolts and nuts. All structural brackets are fastened to the chassis panels with a minimum of three bolts.

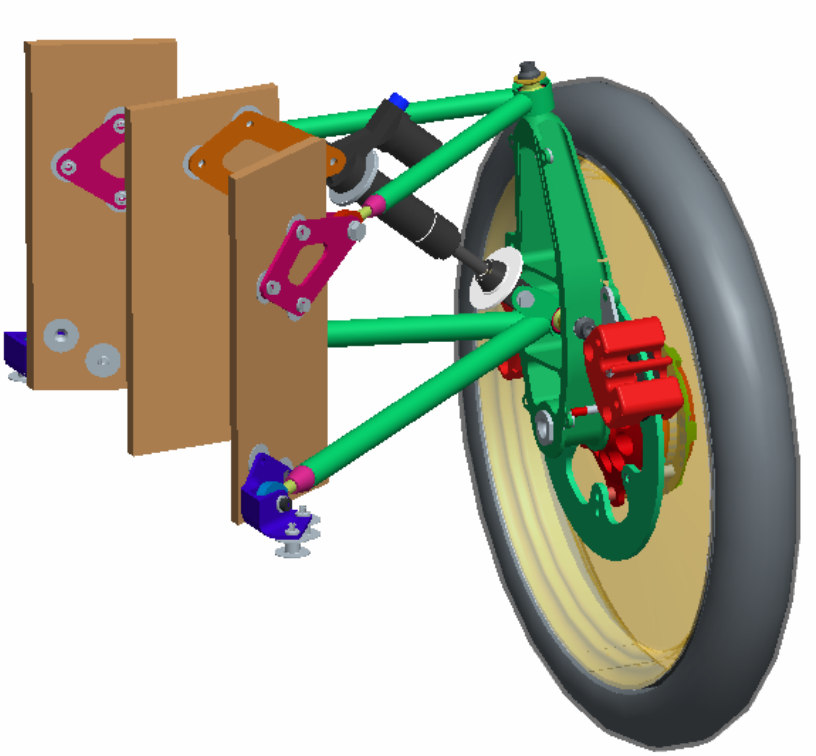

**Figure 2: Front Left Suspension**

## *Rear Suspension*

### Material Specifications

The swing arm assembly is constructed out of 4130 steel tube and plate. The shock links are water-jet cut out of 7075-T6 aluminum. All chassis mounting brackets for rear suspension pieces are made out of 7075-T6 aluminum.

### System Analysis

A Fox spring/shock unit acts directly on the swing arm, with its line of action aimed at the intersection of the arm centerline and the vertical line through the axle. This produces little or no bending moment in the arm due to bump loads. The main load in the arm is torsion with large values produced in bump and cornering. Estimated stresses, using simplified models neglecting additional supports, at critical points were all below yield by safety factors of at least 2.1 for the 1 [G] turn and 4 [G] bump. The upper end of the spring/shock unit is supported by a linkage consisting of two legs of a triangle which connect to the outer ends of the swing arm cross tube with rod ends and a horizontal member with rod ends which attaches to the upper chassis panel, transferring loads directly into the panel. With this arrangement, bump loads at the rear wheel are transferred to the swing arm mounting points, but not through the arm itself. The horizontal member is adjustable for length, which can change rear ride height without using up shock travel. The chassis mounted pivots for the swing arm are

spherical bearings in custom aluminum housings, one on each end of the cross tube. Each housing attaches to two chassis panels with six inserts. Toe and camber adjustment is accomplished by changing a single housing.

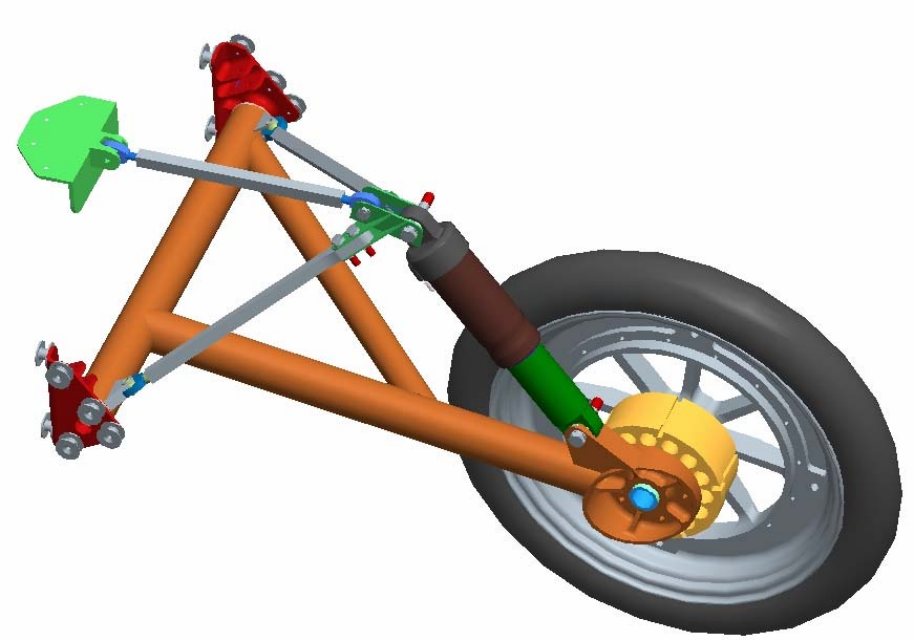

**Figure 3: Rear Suspension**

## *Brakes*

Borealis 3 uses two independent hydraulic braking systems acting at the front wheels, assisted by regenerative braking through the motor at the rear wheel.

### Material Specifications

Each hydraulic system has a master cylinder with a 0.875 [in] diameter piston which actuates two cylinders, one at each front wheel. The master cylinders are supplied from Tolomatic, Inc. The calipers are from Martin Custom Products and have 1.000 [in] diameter pistons. There is a custom 8.000 [in] diameter brake disc at each wheel. The discs are machined from 6061-T6 aluminum and hard coated with “Alpha Coating” from Surface Solutions, Fridley, MN, which provides a surface that is twice the hardness of titanium nitride. A custom pedal assembly actuates both hydraulic systems simultaneously and is adjustable to balance wear on the pads. The regenerative brake is controlled with a lever on the steering wheel. Components were sized based upon an optimistic tire-road coefficient of friction of 1.0, which with front wheel braking only, corresponds to a deceleration of 0.85 [G] using the previous values for wheelbase and CG location. (The value of 1 [G] deceleration shown previously was used for sizing suspension components, but here we need a more realistic value to check pedal force and stresses, and line pressures). A pedal force of 108 [lbf] will supply line pressure of 565 [psi] and produce deceleration of 0.85 [G]. The master cylinders are rated for 1200 [psi]. If one hydraulic system fails the pressure in the

remaining system at 0.85 [G] would double to 1130 [psi] which is still below the rated value. The pedal is constructed from 0.750 [inch] OD by 0.065 [in] wall 4130 steel tubing and its maximum bending stress under this load produces a safety factor of 2.44. It should be pointed out that the rules require a braking deceleration of 0.5 [G], and at this level, the above pedal force and line pressure will reduce and the pedal safety factor would increase.

## *Steering*

### Material Specifications

Directional control of the solar vehicle is accomplished through the use of a rack and pinion steering system. Driver input and system feedback is relayed through a composite fiberglass and foam steering wheel coupled to an aluminum steering shaft. A female steel splined insert mates with a steel pinion splined with the corresponding male pattern. The pinion is coupled to an “Alpha Coated” aluminum rack with a custom aluminum rack and pinion housing bolted to the chassis longitudinal panels. Rack motion is transmitted to the front suspension uprights through an aluminum tie rod, steel rod ends, and aluminum steering arms.

Stock components used for the system include; a steel pinion from Stock Drive Products successfully utilized in our previous four solar vehicles, a steering wheel quick release from Mark Williams Enterprises, Aurora high precision rod ends and bronze bushings from McMaster-CARR. All fastening hardware is aircraft grade AN or NAS series bolts and fasteners. A system overview of the left front wheel is included in figure 4.

### Analysis

System design is optimized for Ackerman steering geometry as well as minimal bump or droop steer. Steering stability is accomplished by a self-righting moment about the kingpin axis from 0.750 [in] each scrub radius and mechanical trail of the tire. Vehicle wheelbase and track dimensions allow for stable maneuvering at high speeds and the ability to pass all dynamic scrutineering requirements.

Loading of the steering system during a 1 [G] corner was used as the worst-case situation for stress on the system. Stress analysis results show safety factors of at least 5.68 on all critical load-bearing components when using 23,000 psi as an estimate for the fatigue strength of 6061-T6 aluminum. Euler buckling calculations show a safety factor of 9.86 for the aluminum tie rods loaded with 100 [lbf] on the outside of a turn.

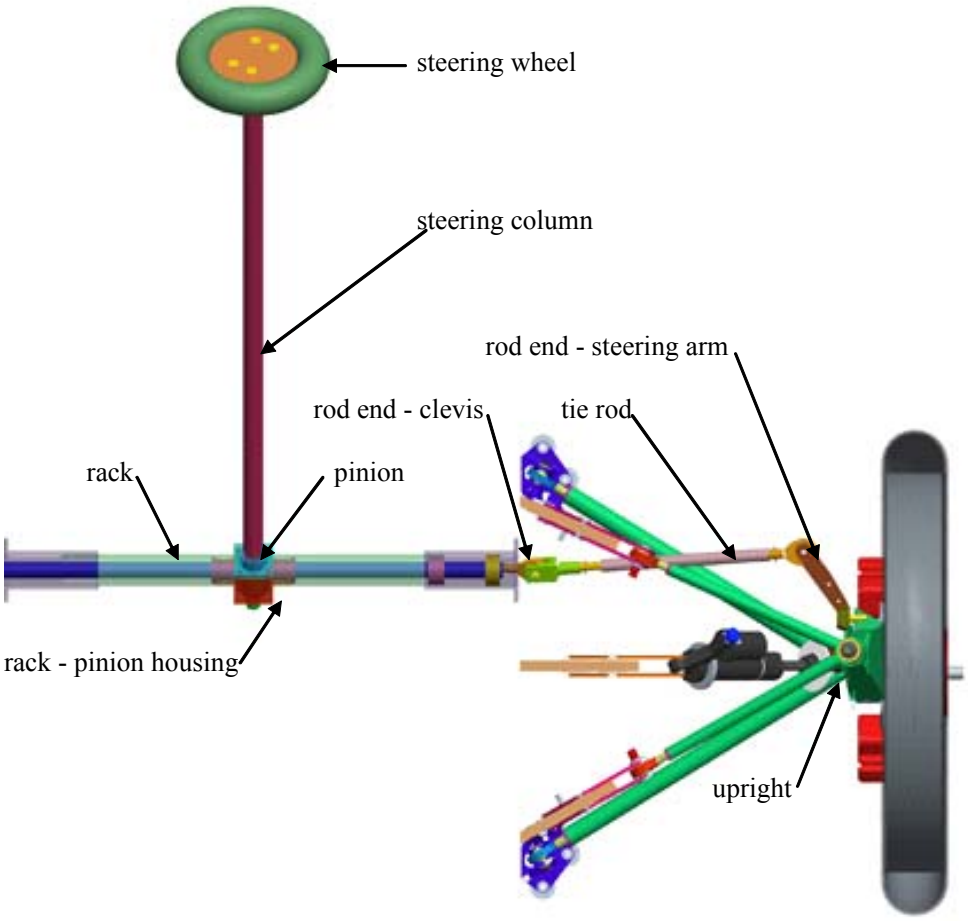


**Figure 4: Top View of Steering System and Front Left Suspension**

## *Wheels and Tires*

Borealis 3 will be using the NGM wheels with Bridgestone Ecopia tires in all races. No further analysis was conducted as it was assumed these commercial components could safely support the vehicle.

## *Battery Enclosure*

The battery box is made of non-conductive 0.400 [in] Hexcel fiberglass composite paneling. The pieces are glued together with non-conductive DP-460 NS two part epoxy. The box is removable and is attached to the car with 6 AN grade grommets and #10 fasteners. The top of the box is removable and is held onto the box with the same grommets and fasteners and will contain the batteries in the box in the case of a vehicle rollover. The front of the box is also removable, but after battery installation, will ideally never have to be removed. It is held onto the box with the same grommets and fasteners. The batteries cells themselves are secured inside the battery enclosure by affixing the cells into

modules using 3M 90 High Strength non-conductive spray adhesive which remains intact up to 71 [C]. Our pack will never reach that temperature, however, since our temperature sensors would shut the car off at 60 [C]. The adhesive has an ultimate shear strength of 230 [psi] and a peel strength of 25 [psi]. These modules are then affixed to a center panel inside the enclosure with the same spray adhesive. The modules will also be protected against vibration by a layer of foam around the outside of the pack. The box will be ventilated using a 12 [V] fan on one side of the box, and a vent on the other side. The fan is exhausted by a duct to the front wheel well.

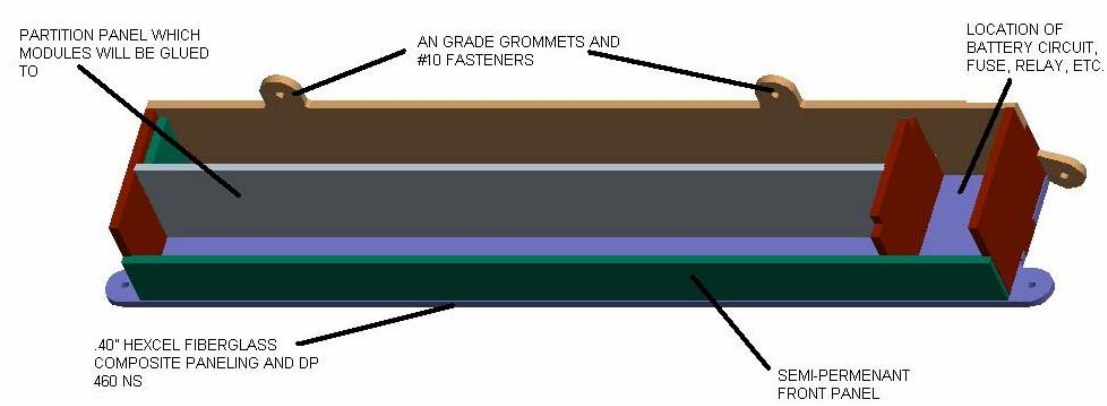


**Figure 5: Battery Box Internals**

# Vehicle Impact Analysis

## *Body Construction*

The body is divided into two separate parts, the bottom and top shells. The bottom shell is mostly structural and is integrated into the chassis. The top shell serves to support the array and act as an aerodynamic shell. For Borealis 3 the top shell was made from aramid prepreg, and the bottom from carbon fiber prepreg. Aramid was chosen for the top because of its non-conductive qualities, light weight, and resistance to shattering. Carbon fiber was chosen for the bottom because of its strength and sandability.

The bottom shell was made at Northwest Airlines Advanced Composite Laboratory. The prepreg chosen for this application was Hexcel BMS 8-168, Type II, Class 2, 3k-70-PW. This is a commonly used 5.7 [oz/sqyd] plain weave carbon fiber with a 250 [°F] cure system resin. Two layers of carbon fiber with an aramid honeycomb core between the layers were used in the lay-up.

The top shell was also made at Northwest Airlines. It was made out of 1.8 ]oz/sqyd] plain weave aramid prepreg, with a 250 [°F] cure system. Four layers of this material were used in the center of the car, while two layers were used near the front and rear extremities. The same aramid honeycomb core used in the bottom shell was used in the top shell.

Three types of core were used in the construction of the nonstructural areas of the bottom shell depending on the severity of the curves in the mold. Plascore PN2 1/4-1.5 aramid honeycomb (hexagonal), 0.250 [in] thickness, 0.250 [in] cell diameter was used on gentle curves and Plascore PN2 1/8-1.8 (flexcore) 0.250 [in] thickness, 0.250 [in] cell diameter was used on the highly curved sides of the vehicle. For the canopy, where it is very difficult to fit core due to the strange curvature, a tulip fiberglass core was used. This small piece was donated by Northwest Airlines, and was much heavier than the aramid core we were using for the rest of the car. Rohacell-31 2.0 lb/cuft core was used on the edges of the car to provide a smooth surface to glue to and to reduce the chances of delamination.

To ensure the rigidity of the shell, a latticework of carbon fiber Fiberlam 2000 bulkheads were glued to the shell. These bulkheads were placed both longitudinally and transversely to the body to ensure even support. They were also designed to help absorb energy in the occurrence of a collision.

**Figure 6: Borealis 3 Shell**

## *Chassis Construction*

The monocoque chassis satisfies the needs of our vehicle far better than other design and construction methods. Monocoque refers to the construction method that directs the forces in the chassis through the skins of the composite material. The carbon fiber paneling we have chosen offers us several advantages over a space-frame chassis. Carbon fiber paneling offers the same lightweight and high strength advantages as an aluminum space-frame design while satisfying several other needs that the chassis must meet. It provides a fully enclosed space for the driver, attachment points for electrical and suspension components, and significantly simplifies construction and design over a space-frame design.

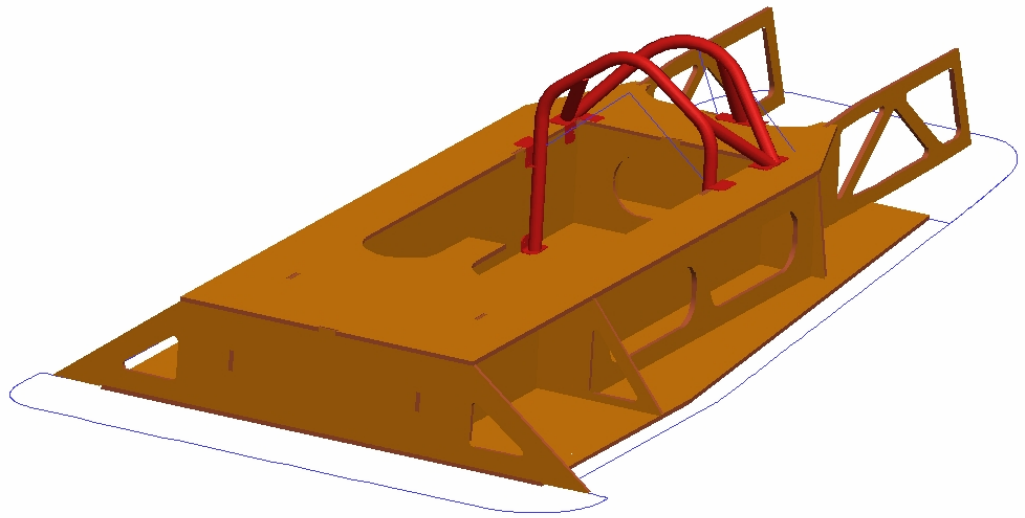

**Figure 7: Chassis and Rollcage**

Carbon fiber paneling owes its great strength to the interlacing fibers in the skins of the paneling. The facing acts like thousands of tiny cables all strung in the same direction held in place by the matrix of resin combined with the facing fabric in it's production. Many fabrics are available, examples being Kevlar, glass, carbon, and Carbon/Kevlar combination. Each has a specific property that is advantageous. Carbon has the highest strength in tension and compression of the materials listed, which is why it was chosen for our highly stressed chassis.

**Figure 8: Completed Chassis at Minnesota's Shop**

The paneling is constructed in a box-beam geometry with panels assembled at 90° to each other which simplifies construction and ensures consistent high quality joints. The panels were designed in such a way that all loads are transferred into the chassis in a direction parallel to at least one prefabricated

panel. The composite panel chassis' were successfully tested with the last five solar cars built, Aurora II, Aurora 3, Aurora IV, Borealis I, and Borealis II.

A mock-up full-scale plywood chassis was constructed before the chassis design was finalized to have model of what the driver cockpit would be like. It helped to integrate the roll bar, pedals, steering, and driver visibility. A complete vehicle assembly in CAD was also used to enhance the integration between all vehicle parts. The combination of these two tools enabled optimal driver placement, layout of components, and integration of vehicle systems.

**Material Specifications**

Hexcel Composites Fiberlam 2000 UD prefabricated paneling was used to construct the majority of the chassis. Theses composite panels are typically used for aircraft flooring. The panels have a thickness of 0.400 [in] consisting of Nomex honeycomb core, cell diameter 0.125 [in], and a nominal thickness of 0.380 [in]. Each side of the core is covered with 2 layers of unidirectional carbon fiber fabric laid perpendicular to each other. Each layer of unidirectional carbon fiber has a thickness of 0.0045 [in]. There is also a .001 [in] thick layer of fiberglass on each side of the paneling to prevent marring and reduce electrical conductivity. The paneling has an average weight of 0.37 [lbm/ft$^2$]. Data from the published four point bending test was used to show a maximum allowable stress in the face sheet of 57,000 [psi].

3MTM Scotch-WeldTM DP-460 NS was used to join the paneling at all joints. This glue is very similar to glue used on previous cars but has a much higher viscosity which assures us that it will not flow away from the joints and will maintain correctly shaped fillets. The epoxy is rated at 4900 [ps]i under the surface preparation conditions used and room temperature curing. The typical joints on the car have approximately 0.400 [in$^2$] of shear area per joint inch. See Figure 9 below. The joint can then be assumed to carry a maximum shear load of (.4inches)(4900psi)=1960 lbf per inch of joint.

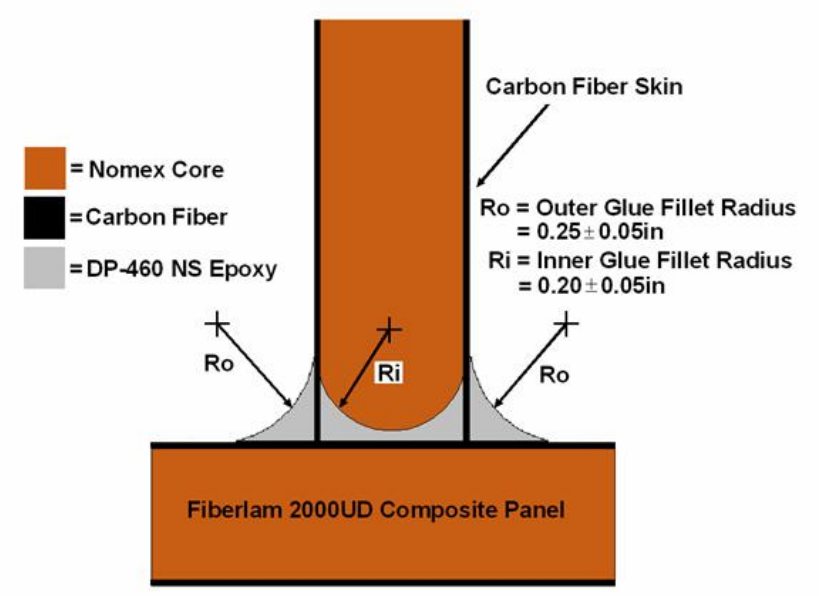


**Figure 9: Chassis Joint Bond**

## Construction

The process used to machine the 4.0 [ft] by 12.0 [ft] Hexcel panels was a water jet cutting machine. This process uses a high-pressure stream of water combined with a garnet aggregate to erode away the material it cuts. The mixture of water and garnet is pressurezed to 40,000 [psi] and focused through a carbide tip into a beam that is .042 [in] in diameter. The water jet tool is the best suited tool for cutting this type of carbon fiber paneling because there is no clamping needed, no carbon fibers released into the air, no forces exerted on the material by the tooling, and it cuts to very high tolerances.

The paneling was placed on a bed of plastic/cardboard energy absorbing material, which is above a steel water tank. The paneling was held in place by its own weight, no clamping was necessary. After the paneling was cut it was quickly cleaned off and dried to prevent delaminating. The paneling was also laid out in a warm dry environment for two days to ensure all the moisture was removed from the paneling before it was glued together.

The paneling was prepped by abrading all glue surfaces followed by extensive cleaning of the glue joints with isopropyl alcohol. Using 3MTM Scotch-WeldTM DP-460 NS two part epoxy the composite paneling was assembled. The epoxy was applied using the 400 [ml] Pneumatic Thunder Epoxy dispenser adapted with 10mm deluxe mixing tips to ensure complete mixing between the resin and the hardener. The epoxy was filleted with a 0.250 [in] radius on the joints, which adequately transfers the forces from one panel to the next as if the chassis was a unified piece. Many of the chassis joints are also reinforced by attachment of the roll bar, suspension, and other components on the car.

### Crush Space

In the event of a collision, a system of progressive safety features will prevent the driver from being injured. The Borealis 3 design places the driver within a safety capsule, with no part of his or her body extending beyond the structural chassis. The driver's shoulders are positioned below the upper plane of the chassis, such that, the torso, containing most vital organs, is located in the center of the structural chassis. The driver's head will be encompassed by a roll cage structure designed to protect the vulnerable driver's head which protrudes through the car's body.

ASC rules require 5.9 [in] of horizontal distance between the diver's shoulders, hips and feet and the car's outer body surface. Borealis 3's minimum crush space of greater than 2 [in] is over four times that required by ASC rules. This large crush space around the driver was made possible by locating the cockpit in a central location in the car. In a rear collision, the 8 [in] of solar car behind the driver will act to absorb much of the impact energy. Likewise, in side collisions the driver resides in the center 20 [in] of the 5.9 [ft] wide car, allowing over 2 [ft] of crush zone on either side. The shell material will crush and the driver is then protected by the driver's compartment as shown in the various crash analysis sections.

Front crush space was maximized beyond race rule requirements with 27.9 [in] of crush space. The 27.9 [in] nose of the car will crush easily, allowing the crash to be stopped by the structural chassis. The front batteries will help block penetrating objects and decelerate the impacting body due to their mass.

## *Driver Restraint Description*

### Drivers Compartment

The driver's safety capsule is designed to remain un-violated in the event of a collision and constrain the driver inside. The 20.0 [in] driver's compartment width holds most drivers snug from left to right which would be beneficial in a side impact. Also, the drivers lower extremities are confined within the drivers compartment from all sides and cannot "flail" in an accident. The side panels are 10.7 [in] high at the driver's shoulders, and when belted in, only the driver's head is above the upper plane of the chassis. The driver head is constrained from moving rearward during a rear impact by a padded headrest. This reduces the risk of a whiplash injury.

### Safety Harness

A six point safety harness will be utilized in Borealis 3. The rear harness attachment points are combined with the roll cage and at the intersection of two or more chassis panels, providing strength in multiple directions. The front

harness attachment is at the lower intersection of two chassis body panels. The driver is reclined at approximately 27 degrees from horizontal. This configuration is similar to that addressed in SAE's Baja Buggy Competition Rules. These rules provided a guideline for harness mounting point location. The shoulder belts are secured below the top of the shoulder, constraining the driver in the event of a roll over. The lap belts are positioned three inches ahead of the intersection of the belly pan and the seat back. This ensures that the belts cross the hips and not the lower abdominal region. The submarine belts secure to the same location holding the driver in a frontal collision. The mounting brackets are bolted through he composite using composite inserts to distribute loads and transfer them to the panels.

## *Roll Cage*

The roll cage is comprised of four components:

-A main hoop in front of the driver, with legs that extend down to the bottom of the chassis. It is attached to the chassis at the bottom edge of the driver compartment (floor of chassis) and the side panels via inserts, along with flanges on the top of the chassis via inserts.
-Two rearward facing supports welded towards the top of the main hoop, and attached to the chassis top and side panels via inserts.
-A rear back-angled hoop behind the driver welded to the same flange as the two rearwards supports and attached to the chassis top and side panels via inserts.
-One rearward facing support welded at the top-center point of the rear hoop and attached to the chassis top panel via inserts.

**Figure 10: Rollcage**

The entire structure is constructed out of 1.250 [in] OD by 0.049 [in] wall 4130 steel tubing and 0.065 [in] 4130 sheet for brackets. The tubing is cold drawn normalized with yield strength reported as 75,000 [psi]. This tubing has an EI stiffness that is 32% larger than that of the 1.000 [in] OD by 0.083 [in] wall tubing as specified in the ASC rules. The larger EI stiffness improves the overall strength, critical buckling load, and crumpling resistance. A professional using the TIG process performed all the welding.

## *Crash Loading Analysis*

### Front and Rear 5 G Collisions

The loading on various panels will be traced and specific joints and panels will be analyzed for strength using accepted procedures based upon the properties of the panels and the bonding agent.

The bumper height ranges from 13.8 [in] to 17.7 [in] and the front chassis lateral bulkhead ranges from 10.5 [in] to 21.5 [in]. Thus the bumper will hit the chassis bulkhead and battery box, once the nose collapses. The body may or may not move rearward as the nose collapses. If the latch and guides for the body fail and the body moves rearward, the drivers canopy will hit the forward roll bar hoop and deflect up and rearward, coming off of the car. The canopy opening extends forward on the body approximately 25 [in] ahead of the driver's head. If the body moves rearward, the edges of the canopy opening will hit the forward roll bar hoop which will either deflect the upper body above the driver, or start tearing the body apart. Eventually, the bumper will contact the battery box and the front chassis bulkhead.

Figure 11 shows a top view of the chassis at this stage, with the inertia forces of the major components:

The front batteries (55 lbm)
The driver (176 lbm)
The body (120 lbm)
The chassis, electrical components and suspension (209 lbm)

Total Weight = 560 lbm

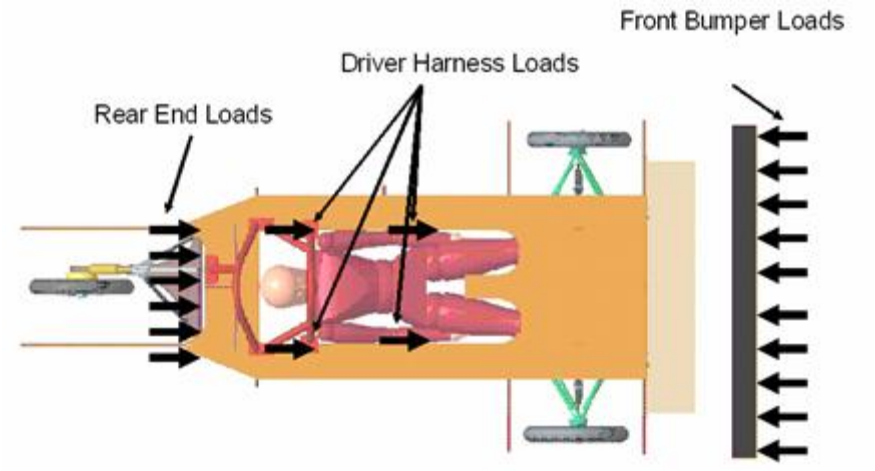


**Figure 11: Assumed Loads in Chassis**

Each of these component weights is multiplied by five to estimate the 5 [G] loading. The center of mass of the front battery pack is within the bumper height, and the battery pack is in front of the front bulkhead, so the inertia force due to the front battery pack acts directly upon the bumper. It does not load the chassis in front end collision. Thus the load on the chassis can be reduced by the 5 [G] force on the front battery pack i.e. Force from bumper upon chassis = 5•(550-55)=5•(495)=2475 lbs (We will use 2500 lb). This load will be initially felt by the two vertical panels, one on each side of the driver. The front chassis bulkhead is glued to these panels, and so will distribute the bumper load across the front vertical face of each panel as shown in Figure 12.

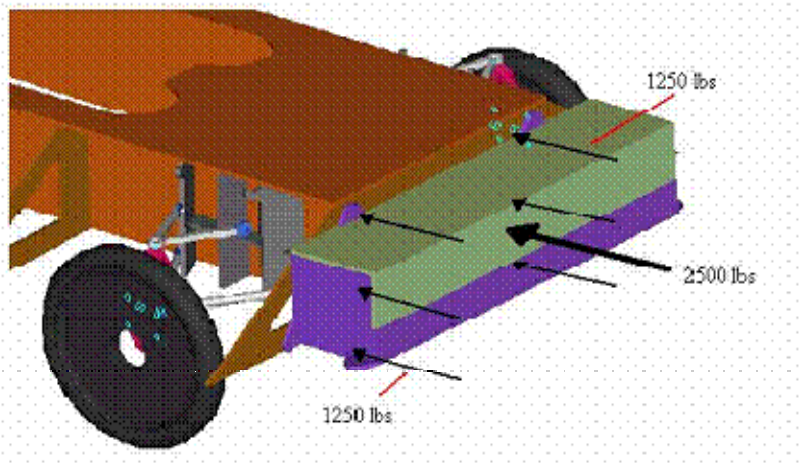


**Figure 12: Net Bumper Loads on Vertical Panels**

The following will argue that the forces are taken by these vertical panels and have sufficient strength to withstand the front bumper loads under very conservative assumptions. The upper and lower panels are used to proved edge stability to the vertical panels and are not figured into the crash analysis. The inertia forces on the driver, body and chassis will all be assumed to be located at the rear of the driver's compartment, and will only be resisted longitudinally by

the two vertical panels. These panels are a minimum of 10 [in] high and 68 [in] long. This is a conservative estimate because some of the impact force would be transmitted to the upper and lower panels as well as the vertical panels.

Each panel of Figure 13 has similar loading, so only one will be examined. The presumed mode of failure is buckling, and the critical stress level can be found using the methods in Successful Composite Techniques, by K. Noakes, Osprey Publishing, 1992, p 133-141.

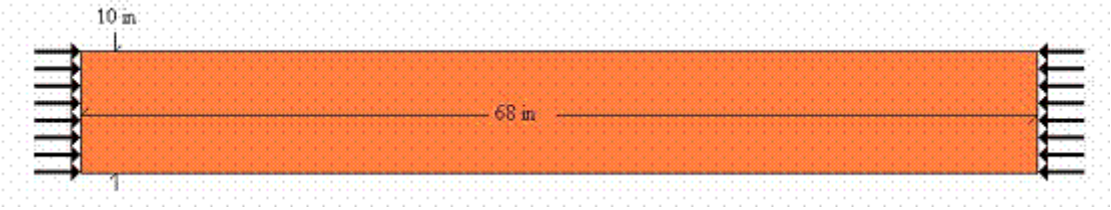


**Figure 13: Assumed Load on Vertical Panels**

When conservatively treated with simply supported edges, the buckling stress in the face sheets was calculated to be 199,859 [ps]i. This figure greatly exceeds the maximum skin stress of 57,000 [psi] as determined from the panel specifications, so in the following, we will use the lower 57,000 [psi] stress level. The actual compressive stress in the skin is simply the 1250 [lbf] load divided by the skin area which gives a compressive stress of 6,250 [psi]. This is far below the 57,000 psi maximum value, giving a safety factor of 9. Thus the driver's compartment can easily withstand the 5 [G] frontal impact.

**Rear Impact**

The trailing edge of the vehicle at nominal ride height is 15.7 [in], while the bumper ranges from 13.8 [in] to 17.7 [in]. Upon impact, the bumper will strike the tail section of the body which will start to collapse and be driven forward. The roll bar has one rearward sloping support which will serve to tear apart the rear body shell before it could impact the driver's headrest, or to drive the body up and over the driver's head. Then the bumper will hit the rear wheel, which has a radius of 9.5 [in], while the rear of the chassis is about 12 [in] above the ground. The bumper will hit the rear wheel above its axle line, thereby pushing it forward and downward. The spring-shock unit will reach its full extension and sever, while the suspension, wheel and motor will be forced below the vehicle chassis as the suspension rod ends fail, being rotated beyond their design limits without the constraint of the shock unit. Finally the bumper will contact the rear chassis bulkhead the same way as for the front impact. The bulkhead will distribute the load to the two longitudinal vertical panels. It has already been shown that these vertical panels can easily handle this 5 [G] impact. The only difference here is the added front battery pack inertial loading. This creates an inertial loading of approximately 2,750 [lbf] and a safety factor of 7. The front battery pack is positioned in front of the front bulkhead and is 36 [in] wide. This is wider than the two vertical panels are apart which means these panels will stop the battery

pack. Thus we can conclude the chassis will withstand both front and rear 5 [G] impacts with the specified bumper.

### Bending Rigidity

To assess the side impact and rollover strength of the chassis, it is necessary to estimate the bending moments caused by inertial loads of the components, and the locations of the chassis supports. The appendix shows the estimated location and weights of components, which can be considered a 1 [G] load. The supports are the rear structural chassis plane and the front axle line. The maximum bending moment due to the loads and supports is seen to be 7071 [in-lbf], occurring in the driver's compartment. The Appendix also shows computation of the chassis moments of inertia about a horizontal axis and vertical axis through the driver's compartment. This data will be used in the side impact and rollover analysis.

### Side Impact at 5 G

This will be treated similarly to the front/rear end collisions. The driver is within the center 20 [in] of the 28 [in] wide structural chassis, with the forward roll bar hoop ahead of the driver's head, and fore-aft supports on each side cradling the driver's head, and a rearl roll hoop behind the driver's head, with a single reward support. The side impact will be considered a plane which contacts the vehicle, crushing the over 20 [in] of body and array before impacting the structural chassis. The canopy would contact the forward hoop and fly off, and the body, which angles upward toward the driver from the side, would slide upward along the roll bar hoops and/or tear itself apart on the roll bar and the fore and aft supports. Eventually the side of the chassis would be contacted.

The load analysis in the appendix can apply here, by presuming that the front and roll bar bulkheads are the supports. This would move the supports closer together reducing the maximum bending moment, so by presuming the maximum 1 [G] bending moment is still about 7000 [in-lbf] to be conservative, a 5 [G] load would give a 35,000 [in-lbf] moment. The maximum bending stress is 1880.6 [psi], well below the allowable 57,000 [psi].

## *Rollover Scenario*

When the vehicle is in a rollover condition, the roll bar and the front of the chassis will support it. The following will show that the roll bar structure is able to support the entire 3 [G] load at various angles. This result will be used to argue that such loads may be placed upon the chassis to determine its strength in bending due to rollover. In the following, it will be shown that the main loop alone is able to withstand that vertical and angular side loads in the plane of the hoop. Then it will be shown that the rearward supports and the main hoop, without the forward tubes, are sufficient to support the front-to-rear loads. Then any combination of

load between these extremes will reduce to these individual loads and hence be accommodated.

**Main Hoop Loads**

The main hoop of the roll bar was analyzed in three loading conditions. These were analyzed using Roark's Formulas for Stress and Strain, Sixth Edition, 1989, Curved Beam Formula 5c, Table 18, p 293-294. These formulas identify the ground loading and moments, which in turn can be used to find the maximum stress. Using the 3 [G] load of f = 1650 [lbf] (550 lbm car) the maximum stress occurs in the attachment area where the hoop crosses that upper chassis plane. The hoop is attached to the chassis with brackets holding 4 inserts on each leg, 2 going into the chassis bottom panel and 2 into the side vertical bulkhead (reinforcing the bonded joint). Also a flange is welded where each leg crosses the upper chassis plane, and 2 more inserts are placed into the side and top panels of the chassis. The stresses due to bending are much larger than due to shear or vertical loading below.

1650 [lbf] vertical load on top of main hoop: max stress = 31,609 [psi]
1650 [lbf] load at 30° on main hoop: max stress = 61,972 [psi]
1650 [lbf] load at 60° on main hoop: max stress = 66,646 [psi]

These are all below the yield stress of 75,000 [psi] for the 4130 CDN steel tube. It must be emphasized that the rearward supports play no role in this analysis, so it is conservative. Since these loads do not have fatigue considerations, the small safety factors are not a concern.

**Fore-Aft Loading of the Roll Bar**

The appendix shows 3 loading cases, in which the rear supports play a role. Each support is an intermediate column with a low L/r ratio and is in the Johnson theory range. It is shown that the safety factors for the fore-aft load cases exceed 13, based upon the yield strength.

Also taken into consideration is that the forward hoop experiences bending stress when a fore-aft load is placed upon the roll cage. This is due to the fact that the two rearward facing supports are welded to the forward hoop about ¾ of the way up the forward hoop. When these cases were analyzed it was found that the safety factors exceed 1.3 in all cases. Again since the loads do not have fatigue considerations and the other components of the roll cage are not considered in the analysis, the small safety factors are not a concern.

Thus it can be concluded that loads placed upon the roll bar structure are transmitted to the chassis structure without causing failure to the roll bar. These loads can be used to determine chassis strength in rollover.

# Appendix

### *Chassis*

Material properties of Hexcel Fibrelam 2000 paneling:

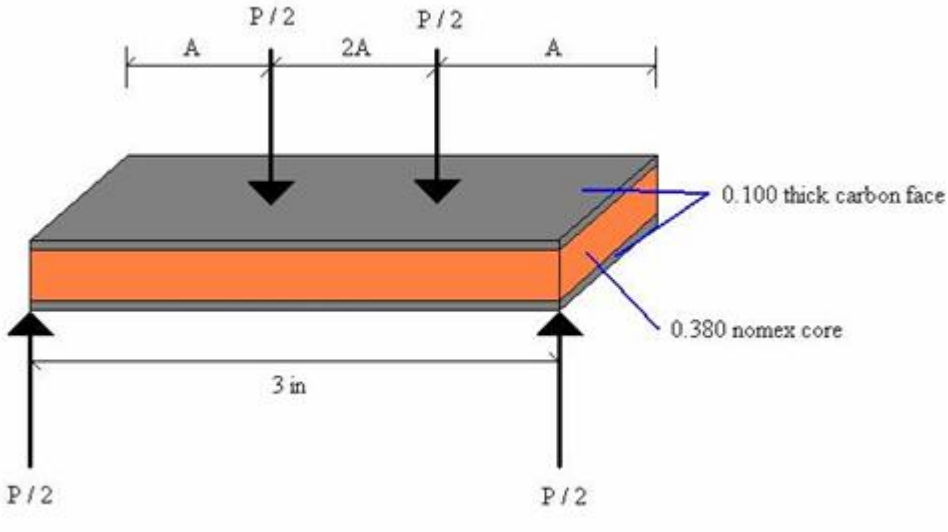


**Figure 14: Four point bending test diagram and data**

P = 260 lbs  A = 5 in.

Critical stress:

Maximum moment is constant and equals $\left(\frac{P}{2}\right)\bullet(A)$
Mmax = P / 2A = (260 / 2)5 = 650 in lbs

Ix = I0.4 - I 0.380 = .00228 in4

$\sigma$crit = - Mmax*y / Ix = 650 * .2 / .00228
$\sigma$crit = 57,020 psi

57,000 psi will be used in the computations.

Chassis beam bending calculations as viewed from right side of vehicle

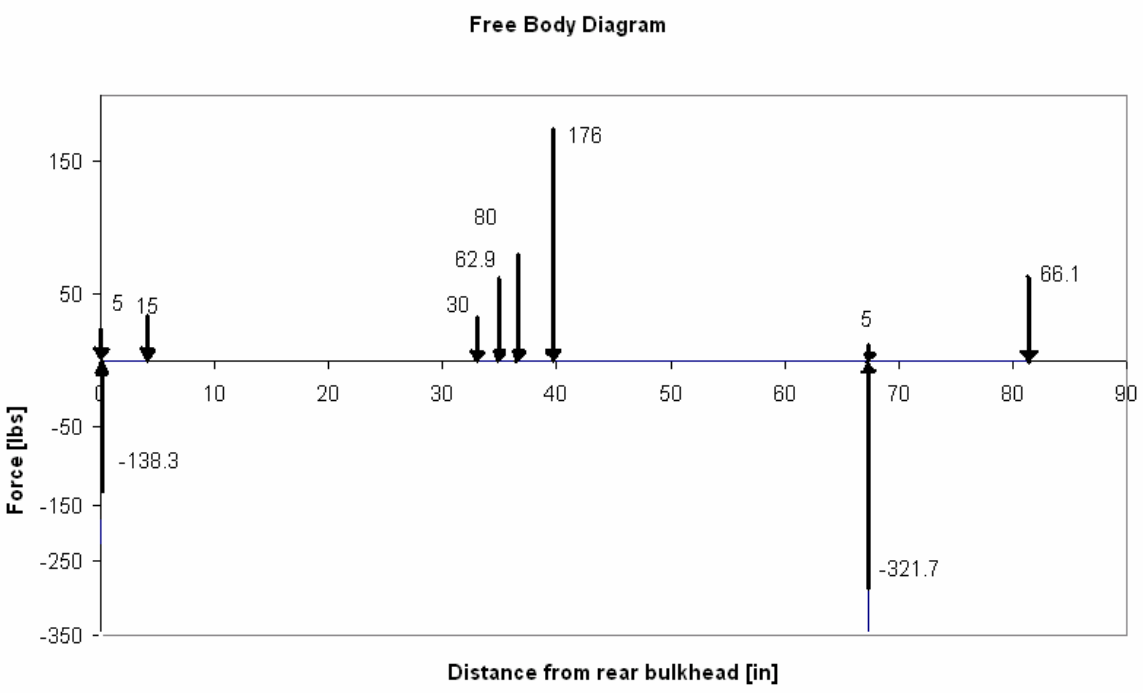


**Figure 15: Chassis Free Body Diagram**

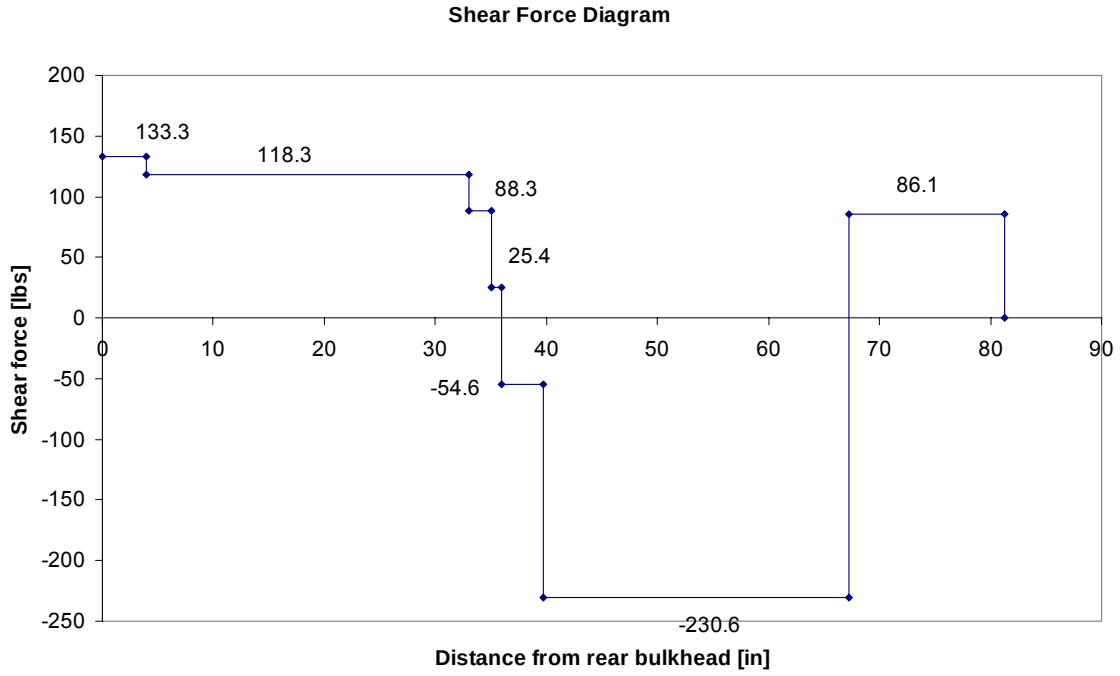


**Figure 16: Chassis Shear Force Diagram**

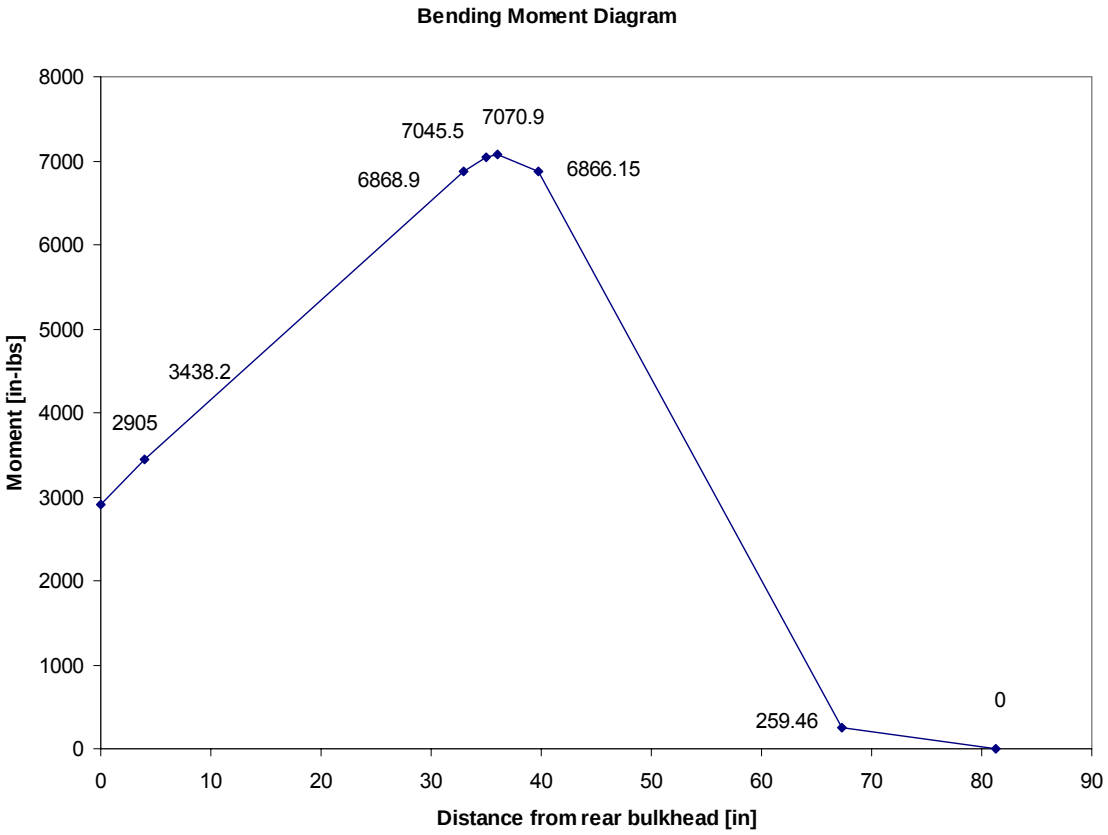


**Figure 17: Chassis Bending Moment Diagram**

**Chassis neutral axis and moments of inertia at maximum moment:**

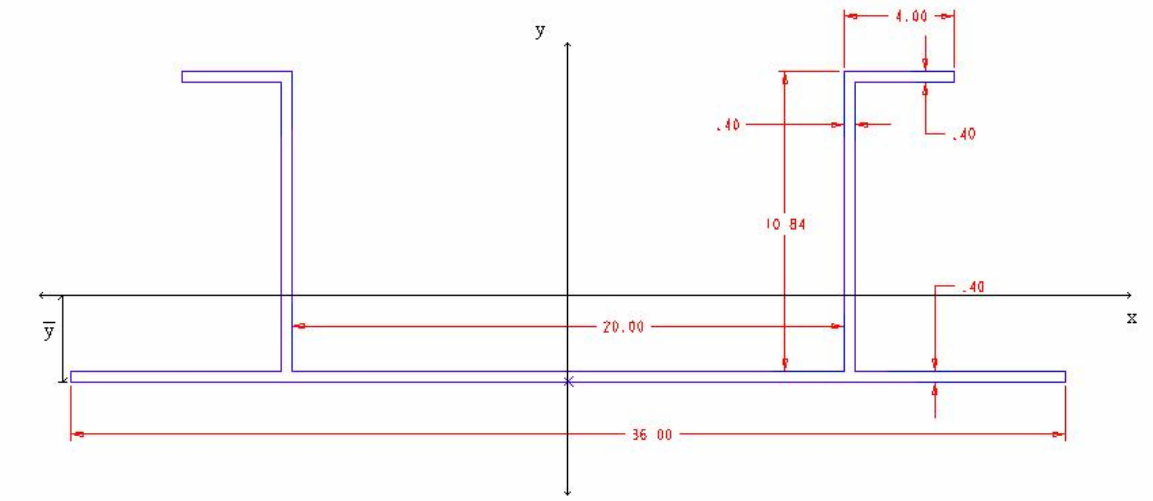


**Figure 18: Chassis Neutral Axis and Moments of Inertia at Maximum Moment**

$\bar{y} = 0.452\ in$

$I_x = \Sigma (I_n + R^2 * A)$
$\underline{I_x = 23.6\ in^4}$

$\bar{x} = 36 / 2 = 18.0$ in

$I_y = \Sigma (I_n + R^2 * A)$
$\underline{I_y = 172.2\ in^4}$

**Maximum stress in chassis paneling:**

$\sigma_{max} = - M_{max} * y / I_x = -7070.9 * 8.216 / 22.6$
$\sigma_{max} =$ 2461 psi / g compression

**Chassis safety factor:**

C.S.F. = $\sigma_{crit} / \sigma_{max}$
C.S.F. = 57,000 psi / 2,461 psi / g = <u>23.16 g</u>

## *Front Suspension Stress Analysis*

### System Analysis

The first step in design was to free body diagram the a-arms and the upright to trace input forces from the tire contact patch all the way to the chassis mountings. The highest forces in the system were found to be approximately 1500 lbf in the front lower a-arm, and 1000 lbf in the top rear a-arm.

Bending moments in the front upright structures were next calculated and used to design upright cross-sections with suitable moments of inertia. This entailed yielding safety factors greater than 1 with respect to aluminum 7075-T6 fatigue strength, and greater than 4 with respect to yield strength under all loading cases. Both of the criteria were satisfied.

Last, buckling calculations were done to prove that our current a-arm designs would not fail under load. For both a-arm, the Johnson mode of buckling was found to be applicable. Using the maximum loads from the force analysis, safety factors of 3.68 for the lower a-arm and 5.33 for the upper a-arm were found. Note tubing wall thickness for lower and upper a-arm used in calculation, 0.049”, is smaller than actual 0.058” wall of the part, therefore safety factor is actually greater than listed calculated value.

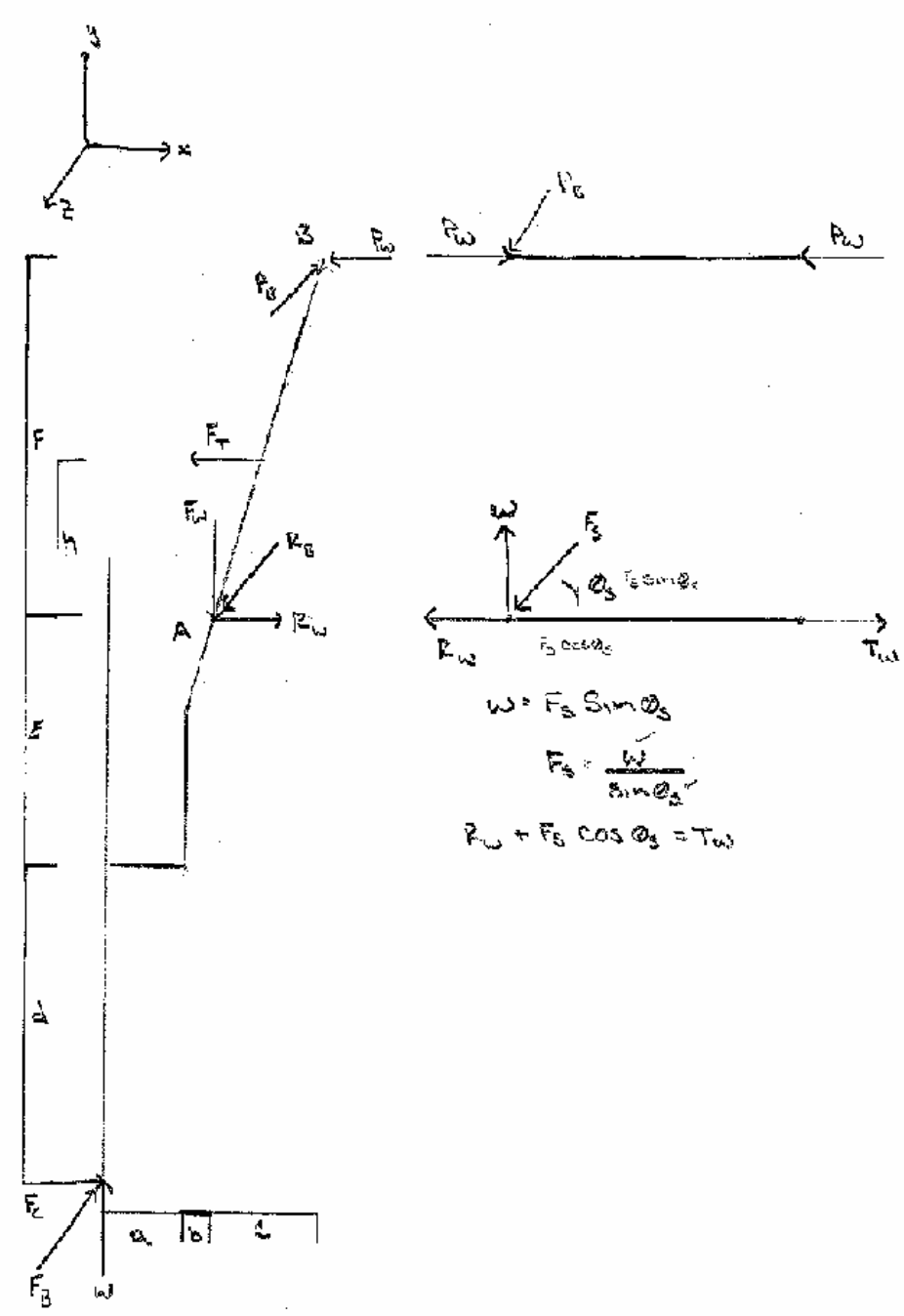


**Figure 19: Front Suspension Free Body Diagram**

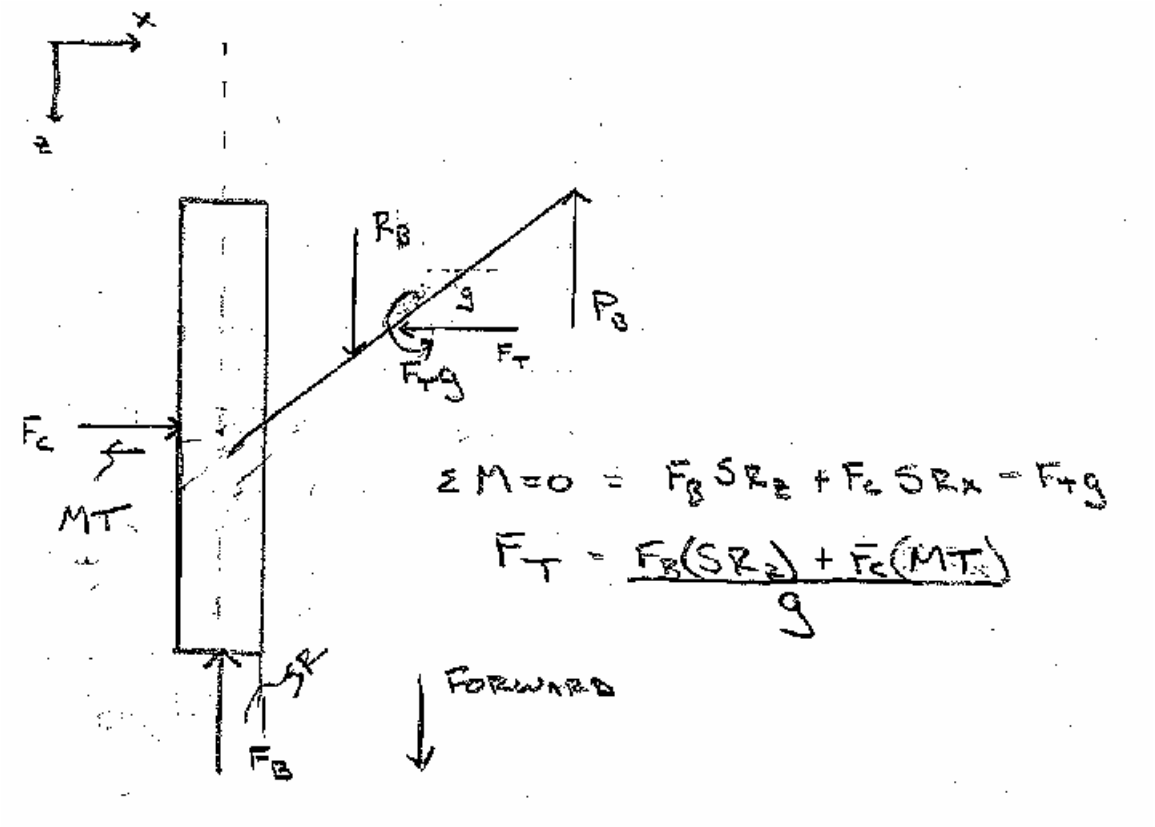


**Figure 20: Front Suspension Free Body Diagram, 2**

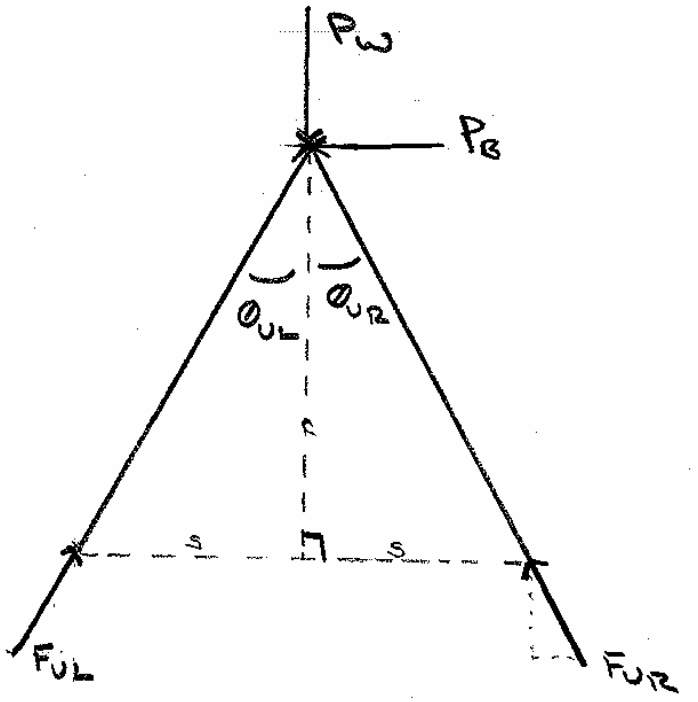


**Figure 21: Upper A-arm Free Body Diagram**

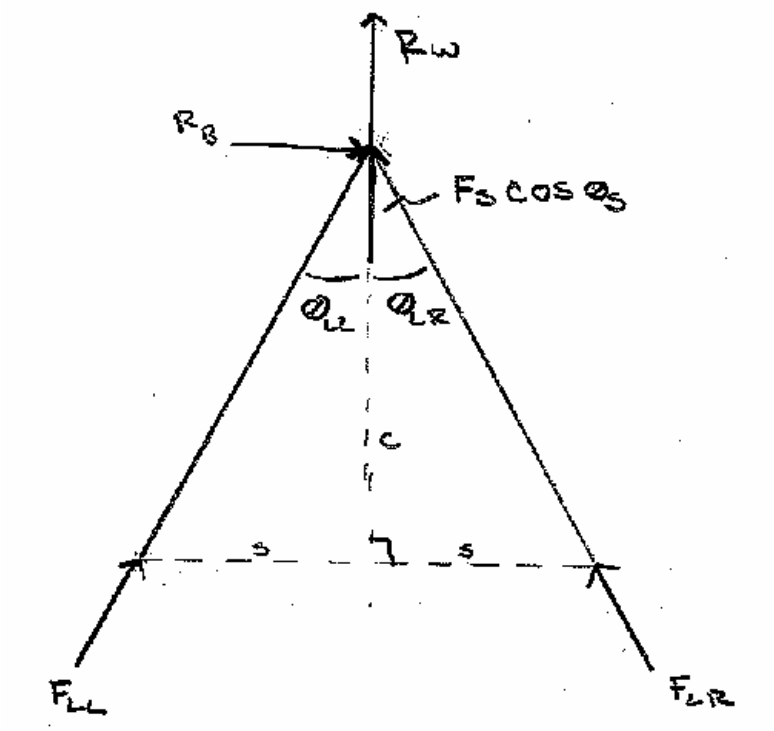


**Figure 22: Lower A-arm Free Body Diagram**

**Table 1: Composition of Forces on One Wheel**

***Composition of Inputs on One Wheel***

***Loading Inputs on Wheel***

Weight Distribution

| | | | | | | | | | |
|---|---|---|---|---|---|---|---|---|---|
| $F_B$ | 0 | 0 | 0.5 | 0.5 | 0 | 0.5 | 0.5 | 0 | (%W) |
| W | 0.33 | 1.33 | 1.33 | 1.33 | 1.33 | 0.33 | 0.33 | 0.33 | |
| $F_C$ | 0 | 0 | 0 | 0.67 | 0.67 | 0 | 0.67 | 0.67 | |

Loading Condition

| | | | | | | | | | |
|---|---|---|---|---|---|---|---|---|---|
| $F_B$ | 0 | 0 | 1 | 1 | 0 | 1 | 1 | 0 | (G's) |
| W | 1 | 4 | 4 | 4 | 4 | 1 | 1 | 1 | |
| $F_C$ | 0 | 0 | 0 | 1 | 1 | 0 | 1 | 1 | |

***Reaction Forces***

| | | | | | | | | |
|---|---|---|---|---|---|---|---|---|
| $P_W$ | 59 | 237 | 230 | -499 | -492 | 52 | -678 | -670 |
| $R_W$ | 59 | 237 | 278 | -751 | -791 | 99 | -929 | -969 |
| $F_S$ | 293 | 1173 | 1173 | 1173 | 1173 | 293 | 293 | 293 |
| $F_W$ | 183 | 733 | 733 | 733 | 733 | 183 | 183 | 183 |
| $P_B$ | 0 | 0 | 539 | 539 | 0 | 539 | 539 | 0 |
| $R_B$ | 0 | 0 | 814 | 814 | 0 | 814 | 814 | 0 |
| $F_T$ | 0 | 0 | 48 | 115 | 67 | 48 | 115 | 67 |

| | | | | | | | | |
|---|---|---|---|---|---|---|---|---|
| $F_{UL}$ | 34 | 137 | 671 | 250 | -284 | 569 | 148 | -387 |
| $F_{UR}$ | 34 | 137 | -406 | -827 | -284 | -509 | **-930** | -387 |
| $F_{LR}$ | -166 | -666 | 125 | 719 | -72 | 624 | 1218 | 427 |
| $F_{LL}$ | -166 | -666 | **-1503** | -909 | -72 | -1003 | -409 | 427 |

| | | | | | | |
|---|---|---|---|---|---|---|
| $\theta_S$ | 0.675 | Radians | 38.680 | Degrees | **Max Upper A-Arm Force** | 930 |
| $\theta_{UR}$ | 0.524 | Radians | 30 | Degrees | **Max Lower A-Arm Force** | 1503 |
| $\theta_{UL}$ | 0.524 | Radians | 30 | Degrees | | |
| $\theta_{LR}$ | 0.524 | Radians | 30 | Degrees | | |
| $\theta_{LL}$ | 0.524 | Radians | 30 | Degrees | | |

***Inputs***

| | | |
|---|---|---|
| Braking 1G | 550 | $F_B$ |
| Static Weight 1G | 550 | W |
| Bump 4G | 2200 | W |
| Cornering 1 G | 550 | $F_C$ |

*Lengths:*

| Name | Value [in] |
|---|---|
| *a* | 1.900 |
| b | 0.188 |
| c | 0.564 |
| total | 2.652 |

*Heights:*

| Name | Value [in] |
|---|---|
| *d* | 9.545 |
| e | 3.087 |
| f | 6.448 |
| total | 19.080 |

*Steering Dimensions:*

| | |
|---|---|
| g | 4.568 |
| SR | 0.795 |
| MT | 0.835 |
| h | 1.043 |

Variables List
li = Length of and individual section
wi = Width of individual section
dxxi = Centroid of individual section in x-direction
dzzi = Centroid of individual section in z-direction
Ixi = Moment of inertia contributed about axis x-x by individual section
Izi = Moment of inertia contributed about z-z by individual section
Ai = Individual section 2-D area

There are four section types in the upright cross section
1-Horizontal Center, 2-Vertical Sides, 3-Open-Side Flanges, 4-Closed-Side Flanges

Section Centriods
Subscript 'i' refers to which section type is being calculated for.

$$\bar{x}_{total} = \frac{\sum\left(\bar{x}_i \cdot A_i\right)}{\sum A_i}$$

By symmetry of the cross section, we know that the centroid in the z-direction will be exactly in the middle.

$$\bar{z}_{total} = \frac{\sum\left(\bar{z}_i \cdot A_i\right)}{\sum A_i} = 0$$

$$dzz_1 = \bar{x}_{total} - \bar{x}_1$$

dxxi and dzzi vary for each section type

Parallel Axis Theorem: ex: $Ix_1 = \frac{l_3^3 \cdot w_4}{12} + A_1 \cdot dxx_1^2$

Total Moments of Inertia

$$Iz_{total} = \sum Izi$$

$$Ix_{total} = \sum Ixi$$

Bending Stress and Bending Stress Distance
Since there is bending acting in two different planes (xy and yz) it is not totally accurate to find a safety factor for each plane and report just those. To be more accurate the total bending moment was found by using the RSS method. The angle between the net bending moment and $M_{yz}$ was also found. The use of Mohr's circle was then introduced to find the x-z combination of inertia that acts along the same line of action as the combined bending stress. The true bending stress can then be found using $M_T$ and $I_{XZ}$. (Mechanics of Materials, Gere, 5th Edition, 2001)

$$M_T = \sqrt{M_{XY} \cdot M_{YZ}}$$

$$\theta_T = ATAN\left(\frac{M_{XY}}{M_{YZ}}\right)$$

$$L_T = \frac{L_4}{2} + L_2$$

$$W_T = \frac{L_T}{Tan(\theta_T)} = \frac{\frac{L_4}{2} + L_2}{Tan(\theta_T)}$$

$$Y_T = \sqrt{\left(\frac{L_4}{2} + L_2\right)^2 + W_T^2}$$

Definition of Stresses Acting

$\sigma_M = \frac{M_T Y_T}{I_{XY}}$ (Bending Stress)

$\sigma_N = \frac{N}{A}$ (Axial Stress)

$\tau_X = \frac{V_{XY}}{A}$ (Shear Stress in xy plane)

$\tau_Y = \frac{V_{YZ}}{A}$ (Shear Stress in yz plane)

$\tau_T = \tau_X - \tau_Y$ (Total Shear Stress)

Using Distortion Energy Theorem

$\sigma_E = \sqrt{\sigma_T^2 + 3\tau_T^2}$

$SF = \frac{S_Y}{\sigma_E}$

Note: 7075-T6 Aluminum Properties: Fatigue Stress = 23000psi @ 500,000,000 Cycles (www.matweb.com), Yield Stress = 70,000psi (Fundamentals of Machine Component Design 3rd, Juvinall and Marshek)

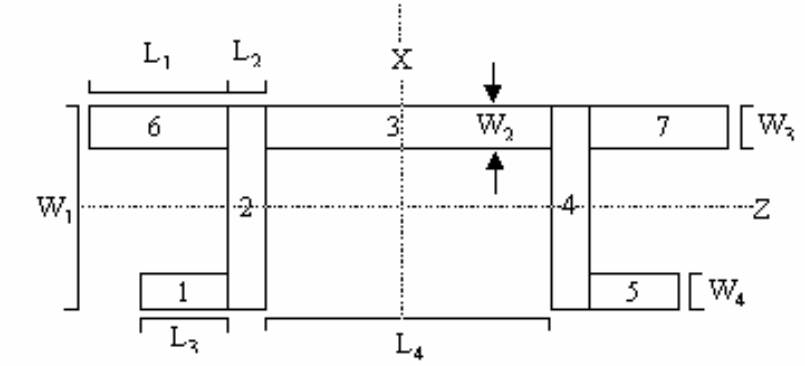


**Figure 23: Upright Cross Section**

## Table 2: Moment of Inertia Calculations for Front Suspension Upright Cross Section at Areas of Direct Load Application

**At Axle Line**

*Cross Section Dimensions*

| | | | |
|---|---|---|---|
| $L_1$ | 0.262 | $W_1$ | 1.5 |
| $L_2$ | 0.125 | $W_2$ | 0.125 |
| $L_3$ | 0.262 | $W_3$ | 0.125 |
| $L_4$ | 1.244 | $W_4$ | 0.125 |

*Moments*

| | |
|---|---|
| IX | 0.392997 |
| IZ | 0.267654 |
| IXZ | 0.615777 |

*Moment Calculations of Sections*

| Section | A | $D_{XX}$ | $D_{ZZ}$ | $I_{iX}$ | $I_{iZ}$ |
|---|---|---|---|---|---|
| 1 & 5 | 0.03275 | 0.878 | 0.6875 | 0.000187 | 4.26E-05 |
| 2 & 4 | 0.1875 | 0.6845 | 0 | 0.000244 | 0.035156 |
| 3 | 0.1555 | 0 | 0.6875 | 0.020053 | 0.000202 |
| 6 & 7 | 0.03275 | 0.878 | 0.6875 | 0.000187 | 4.26E-05 |

**At Lower Joint**

*Cross Section Dimensions*

| | | | |
|---|---|---|---|
| $L_1$ | 0.25 | $W_1$ | 1.5 |
| $L_2$ | 0.125 | $W_2$ | 0.125 |
| $L_3$ | 0.25 | $W_3$ | 0.125 |
| $L_4$ | 2.5 | $W_4$ | 0.125 |

*Moments*

| | |
|---|---|
| IX | 0.843587 |
| IZ | 0.371663 |
| IXZ | 1.053889 |

*Moment Calculations of Sections*

| Section | A | $D_{XX}$ | $D_{ZZ}$ | $I_{iX}$ | $I_{iZ}$ |
|---|---|---|---|---|---|
| 1 & 5 | 0.03125 | 1.5 | 0.6875 | 0.000163 | 4.07E-05 |
| 2 & 4 | 0.1875 | 1.3125 | 0 | 0.000244 | 0.035156 |
| 3 | 0.3125 | 0 | 0.6875 | 0.16276 | 0.000407 |
| 6 & 7 | 0.03125 | 1.5 | 0.6875 | 0.000163 | 4.07E-05 |

**Just Below Upper Joint**

*Cross Section Dimensions*

| | | | |
|---|---|---|---|
| $L_1$ | 0.255 | $W_1$ | 1.017 |
| $L_2$ | 0.125 | $W_2$ | 0.125 |
| $L_3$ | 0.255 | $W_3$ | 0.125 |
| $L_4$ | 1.347 | $W_4$ | 0.125 |

*Moments*

| | |
|---|---|
| IX | 0.331673 |
| IZ | 0.15426 |
| IXZ | 0.31758 |

*Moment Calculations of Sections*

| Section | A | $D_{XX}$ | $D_{ZZ}$ | $I_{iX}$ | $I_{iZ}$ |
|---|---|---|---|---|---|
| 1 & 5 | 0.031875 | 0.926 | 0.446 | 0.000173 | 4.15E-05 |
| 2 & 4 | 0.127125 | 0.736 | 0 | 0.000166 | 0.010957 |
| 3 | 0.168375 | 0 | 0.446 | 0.025458 | 0.000219 |

| | | | | | |
|---|---|---|---|---|---|
| 6 & 7 | 0.031875 | 0.926 | 0.446 | 0.000173 | 4.15E-05 |

**Table 3: Forces and Stress Calculations for Front Suspensions Upright Cross Section at Areas of Direct Load Application**

Forces Acting and Type

| ***XY Plane*** | Bending | Axial | Shear | ***YZ Plane*** | Bending | Axial | Shear |
|---|---|---|---|---|---|---|---|
| Axel | 4893 | 733 | 367 | Axel | 2625 | 733 | -275 |
| Lower A-Arm | 6025 | 733 | -385 | Lower A-Arm | 3473.7313 | 733 | 539 |
| Upper A-Arm | 704 | 0 | -670 | Upper A-Arm | 539 | 0 | 539 |

At Axle Line

| *Determination of Max Stress Point* | | *Max Stresses* | |
|---|---|---|---|
| $M_{XY}$ | 4893 | $\sigma_M$ | 7644 |
| $M_{YZ}$ | 2625 | $\sigma_N$ | 1109 |
| $M_T$ | 5553 | $\sigma_T$ | 8753 |
| $\theta_T$ | 1.078 | | |
| *Distance to Max Stress Point'* | | $\tau_X$ | 554 |
| $W_T$ | 0.4007 | $\tau_Y$ | -416 |
| $Y_T$ | 0.8477 | $\tau_T$ | 970 |

At Lower Joint

| *Determination of Max Stress Point* | | *Max Stresses* | |
|---|---|---|---|
| $M_{XY}$ | 6025 | $\sigma_M$ | 10474 |
| $M_{YZ}$ | 3474 | $\sigma_N$ | 903 |
| $M_T$ | 6955 | $\sigma_T$ | 11376 |
| $\theta_T$ | 1.048 | | |
| *Distance to Max Stress Point'* | | $\tau_X$ | -473 |
| $W_T$ | 0.7928 | $\tau_Y$ | 663 |
| $Y_T$ | 1.5872 | $\tau_T$ | -1136 |

Just Below Upper Joint

| *Determination of Max Stress Point* | | *Max Stresses* | |
|---|---|---|---|
| $M_{XY}$ | 704 | $\sigma_M$ | 2807 |
| $M_{YZ}$ | 539 | $\sigma_N$ | 0 |
| $M_T$ | 887 | $\sigma_T$ | 2807 |
| $\theta_T$ | 0.918 | | |
| *Distance to Max Stress Point'* | | $\tau_X$ | -1218 |
| $W_T$ | 0.6109 | $\tau_Y$ | 979 |
| $Y_T$ | 1.0054 | $\tau_T$ | -2197 |

| Safety Factors | $\sigma_E$ | $\sigma_Y$ | $\sigma_{Y\ Fatigue}$ | $SF_{Actual}$ | $SF_{Fatigue}$ |
|---|---|---|---|---|---|
| Axel | 8912 | 70000 | 23000 | 7.85 | 2.58 |
| Lower Joint | 11545 | 70000 | 23000 | 6.06 | 1.99 |
| Below Upper Joint | 4728 | 70000 | 23000 | 14.80 | 4.86 |

Governing Equations

$$SR_D = \sqrt{\frac{2\pi^2 E}{S_Y}}$$

Slenderness Ration Dividing Line

$$SR = \frac{L_{EQ}}{\sqrt{\frac{I}{A}}}$$

Slenderness Ratio

$$P_{CR} = A_{XSec}\left[S_Y - \frac{S_Y^2}{4\pi^2 E}\left(\frac{L_{EQ}}{\sqrt{\frac{I}{A}}}\right)^2\right]$$

Critical Load for Buckling (Johnson Column)

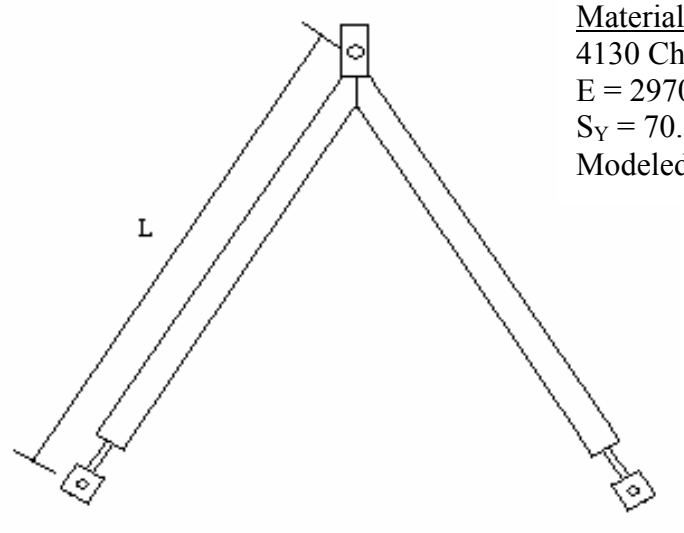


Material Properties
4130 Chromoly Steel Hollow Tubing
E = 29700 ksi (www.matweb.com)
$S_Y$ = 70.0 ksi (www.emjmetals.com)
Modeled as Fixed-Pinned Column

| Location | Dividing Slender | Slender Ratio | Outer Diam (In) | Inner Diam (In) | Wall Thick (In) | Moment Inertia | Cross Area ($In^2$) | Length (In) | F Crit (Lbf) | Max Load (Lbf) | Safety Factor |
|---|---|---|---|---|---|---|---|---|---|---|---|
| Upper A-arm | 96.237 | 46.698 | 0.625 | 0.527 | 0.049 | 0.0037 | 0.0887 | 9.54 | 4952 | 930 | 5.33 |
| Lower A-arm | 96.237 | 59.297 | 0.750 | 0.652 | 0.049 | 0.0067 | 0.1079 | 14.73 | 5534 | 1503 | 3.68 |

## *Rear Suspension Stress Analysis*

### Assumptions

In determining the forces acting on the rear suspension, several assumptions were made. These assumptions were simply the given forces of 187 [lbf] of weight, and 1 [G] cornering force equaling [187 [lb].

### Reaction Forces

The first step in determining the forces in the system was to determining the reaction forces. The free body diagram can be seen in figure 24. In this diagram the vehicle is turning to the right.

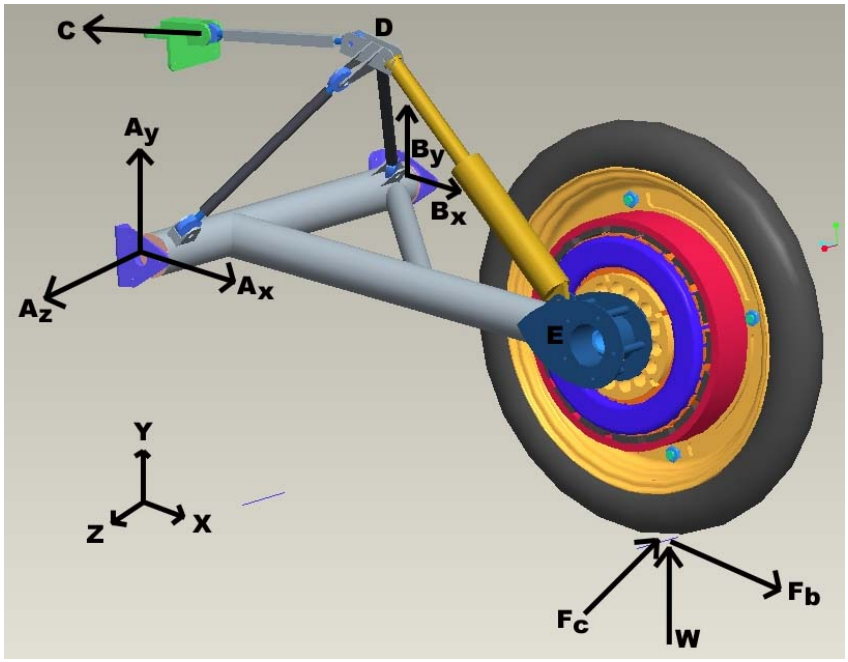


**Figure 24: Rear Suspension Input Forces and Reactions**

To determine the reaction forces, point A was classified as the origin. The dimensions of points B, C, D and E are shown in the following Table 4.

**Table 4: Rear Suspension Dimensions**

| Points | x (in) | y (in) | z (in) |
|---|---|---|---|
| A | 0 | 0 | 0 |
| B | 0 | 0 | -17.4 |
| C | -0.62 | 9.25 | -5.2 |
| D | 9.25 | 9.25 | -5.2 |
| E | 21.02 | -3.77 | -5.2 |

From statics equations, all reaction forces can be found. These statics equations were developed to trace $F_c$ and W back to the points A, B, C and the internal forces. Then a spreadsheet was developed to allow entering different values for braking, cornering, and bump, the worst-case reaction forces were determined. The largest force at point A occurs when the car is experiencing a 4 [G] bump and is cornering at 1 [G] to the left. The result in the driver side mounting bracket is 2000 [lbf] of force at A, with the majority of the force in the negative x direction. The worst case scenario at the passenger side mounting bracket, point B, occurs when the car is experiencing a 4 [G] bump and cornering at 1 [G] to the left. During these conditions, the passenger mounting bracket is subjected to 800 [lbf] of force with a majority of the force in the negative y direction. Loads in the z directions are only felt at point A by design where a snap ring holds the bearing in place. At point B the bearing is allowed to slide in the z direction to that no additional stresses are put on the chassis by holding the swingarm.

The worst case scenario for the upper mounting bracket, point C, occurs when the car experiences a 4 [G] bump. The upper mounting bracket experiences approximately 1700 [lbf] in the negative x direction during these conditions. Cornering has no bearing on the upper mounting bracket. The line of action of this force is pointed parallel to and between the two layers of carbon fiber in the paneling of the chassis.

**Internal Forces**

The bracket that joins all of the 2 force links shown in the Figure is designed so that the line of action of each force meets at point D

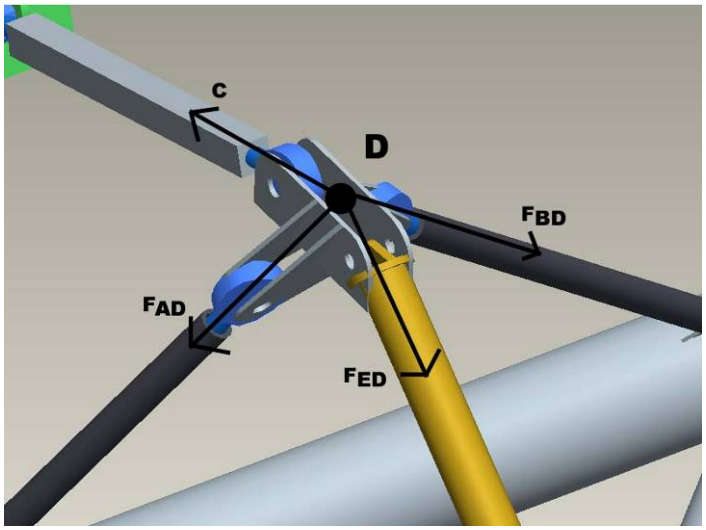


**Figure 25: Internal Forces at Point D**

## Stress Analysis

Stress analysis will be performed for components of the rear suspension which are made of the following materials. The stress analysis will consider a worst case scenario of a 4 [G] bump and 1 [G] cornering. With this type of loading, reaction forces and torques are greatest when the car is cornering to the right. Material Property Information:

7075-T6 Aluminum

| | | | |
|---|---|---|---|
| *Yield Strength* | *Sy=* | *73000* | *[psi]* |

Normalized 4130 Steel

| | | | |
|---|---|---|---|
| *Yield Strength* | *Sy=* | *75000* | *[psi]* |

## Component Stress Analysis

For the following three links, column buckling is a potential result since they experience axial compressive stress for worst case loading.

**Table 5: Column Bulking Safety Factors in Shock Links**

| | Link AD 7075-T6 | Link BD 7075-T6 | Link CD |
|---|---|---|---|
| Material Type: | Al | Al | 7075-T6 |
| Nominal Length (in) | 10.58 | 14.72 | 8.62 |
| Cross-section type | Solid Square | Solid Square | Solid Square |
| Cross-section Area (in2) | 0.25 | 0.25 | 0.25 |
| Cross-sectional moment of inertia (in4) | 0.00521 | 0.00521 | 0.00521 |
| Radius of gyration, ρ | 0.1443 | 0.1443 | 0.1443 |
| Compressive Load (lbf) | 1094.7 | 592.9 | 1699 |
| Resulting Stress | 4378.8 | 2371.6 | 6796 |
| Decision Coefficient, Le/ρ | 73.31 | 102.0 | 59.73 |
| Decision Criteria Coefficient, SR/D = ((2π2E)/Sy)^0.5 | 53.02 | 53.02 | 53.02 |
| Buckling Type | Euler | Euler | Euler |
| Critical Stress, Scr | 19093 | 9863 | 28764 |
| Safety Factor | 3.82 | 7.40 | 4.9 |

## Swing Arm

The tubing of the swing arm experiences the greatest amount of stress is at a point 9 [in] forward from the axle. At this point, tensile, bending, and torsional stresses exist. Each stress component will be calculated, and then the equivalent mean stress at this point will be determined. The actual stress will be compared to the yield strength of 4130 steel in a safety factor calculation.

The tubing of the swing arm has the following geometric properties:

| | |
|---|---|
| Cross-sectional area [$in^2$]: 0.3440 | Torsion [in-lbf]: 4488.4 |
| Cross-sectional moment of Inertia [$in^4$]: 0.1223 | Bending Moment [in-lbf]: 3939.7 |
| Polar moment of Inertia [$in^4$]: 0.2446 | Torsional Stress [psi]: 16057 |
| Outer Diameter [in]: 1.75 | Bending Stress [psi]: 28187 |
| Wall Thickness [in]: .065 | Principal Stress [psi]: 35458 |
| | Safety Factor: 2.11 |

## *Roll Cage Stress Analysis*

### Computation of Stress in Main Roll Bar Hoop

Using Roark's Table 18, "Circular Arches", case 5C

F = 3G load = 3(550) = 1650 lb
R = 10.698 inches

Roark's load case 5C finds the reactions at A fro the following matrix equation:

$$\begin{bmatrix} \frac{\pi}{2} & 2 & \frac{2}{R} \\ 2 & \frac{3\pi}{2} & \frac{\pi}{R} \\ 2 & \pi & \frac{\pi}{R} \end{bmatrix} \begin{bmatrix} H_A \\ V_A \\ M_A \end{bmatrix} = \begin{bmatrix} LF_H \\ LF_V \\ LF_M \end{bmatrix}$$

Reactions at B are found from:

$$V_B = F\cos\phi - V_A, lb$$

$$H_B = F\sin\phi - H_A, lb$$

$$M_B = FR\cos\phi - 2RV_A - M_A, in-lb$$

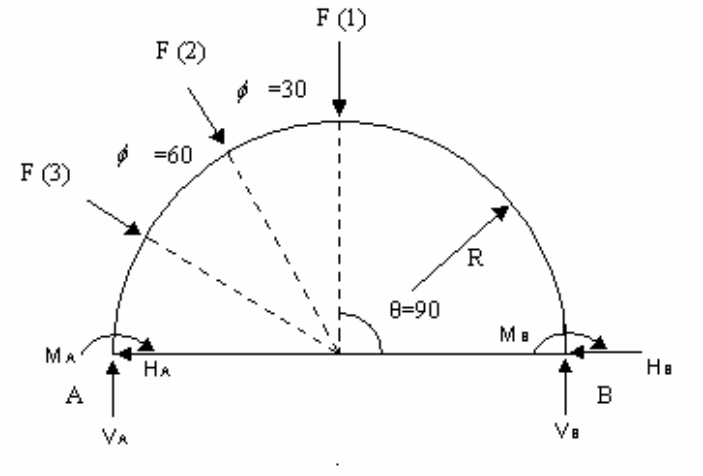


Matrix elements depend on angle θ = 90º and radius R. The "LF" terms depend upon the load F and

Results Summary for 3 Load Cases

| Case | $\phi$ | LFH | LFV | LFM | HA | VA | MA | HB | VB | MB | σB |
|---|---|---|---|---|---|---|---|---|---|---|---|
| 1 | 0 | 825 | 2946 | 1650 | -758 | 825 | 1688 | 758 | 825 | -1688 | 31609 |
| 2 | 30 | 1584 | 3960 | 2475 | 28 | 945 | -1623 | 797 | 484 | -3309 | 61972 |
| 3 | 60 | 2277 | 4158 | 3079 | 1065 | 687 | -3559 | 364 | 138 | -2314 | 66646 |

σB = The Maximum Bending Stress, psi

$$\sigma_B = \frac{Max(M_A, M_B)C}{I}$$

For 1.25" x 0.049" wall tube $\frac{C}{I} = 18.726$

Fore-Aft Loads on Roll Hoop

Consider load F = 1650 lb at angles $0 \le \phi \le 60$ o

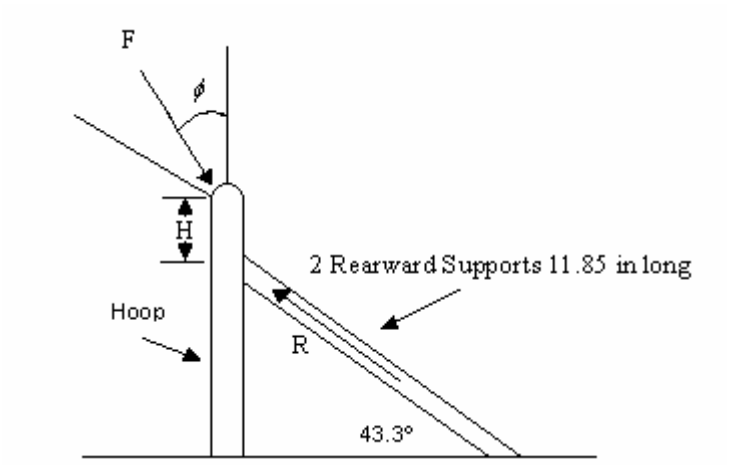


Reactions are assumed to be equally divided between the two supports, each denoted as R. Treat each support as affixed-fixed column (due to welded ends) in compression and find PCRIT.

Tube Properties

$$L_e = \frac{11.85}{2} = 5.93 \text{ inches}$$

$$\text{r} = \text{radius of gryation} = 0.425 \text{ inches}$$

$$\text{Area} = 0.1849 \text{ inches}^2$$

$$E = 30x10^6 \ psi$$

$$\sigma_Y = 75x10^3 \ psi$$

Check to see if Johnson Theory applies

$$\frac{L_e}{r} = 13.94 < \left(\frac{2\pi^2 E}{\sigma_Y}\right)^{\frac{1}{2}} = 89$$ Yes, so:

$$P_{CRIT} = Area\left[\sigma_Y - \frac{\sigma_Y^2}{4\pi^2 E}\left(\frac{L_e}{r}\right)^2\right]$$ =13,697 lb

Define safety factor = $$SF = \frac{P_{CRIT}}{R}$$

| $\phi$ | R | SF | Comments |
|---|---|---|---|
| 0º | 0 | -- | No fore-aft reaction with $\phi$=0 |
| 45º | 802 | 17.09 | Each Support load is (0.5)F |
| 0º< $\phi$ <45º | < 802 | > 13.95 | Support Loads < (0.5)F |
| 60º | 982 | 13.95 | Support Loads = (0.60)F |

Bending Above Weld Points in Main Hoops

$$\sigma_B = \frac{My}{I} = \frac{F_X \cdot H \cdot C}{I}$$

$$SF = \frac{75{,}000\,psi}{\sigma_B}$$

| Case | φ | FX | H | σB | SF |
|---|---|---|---|---|---|
| 1 | 0 | 0 | 4.34 | 0 | -- |
| 2 | 30 | 413 | 4.34 | 33524 | 2.24 |
| 3 | 60 | 714 | 4.34 | 58066 | 1.29 |

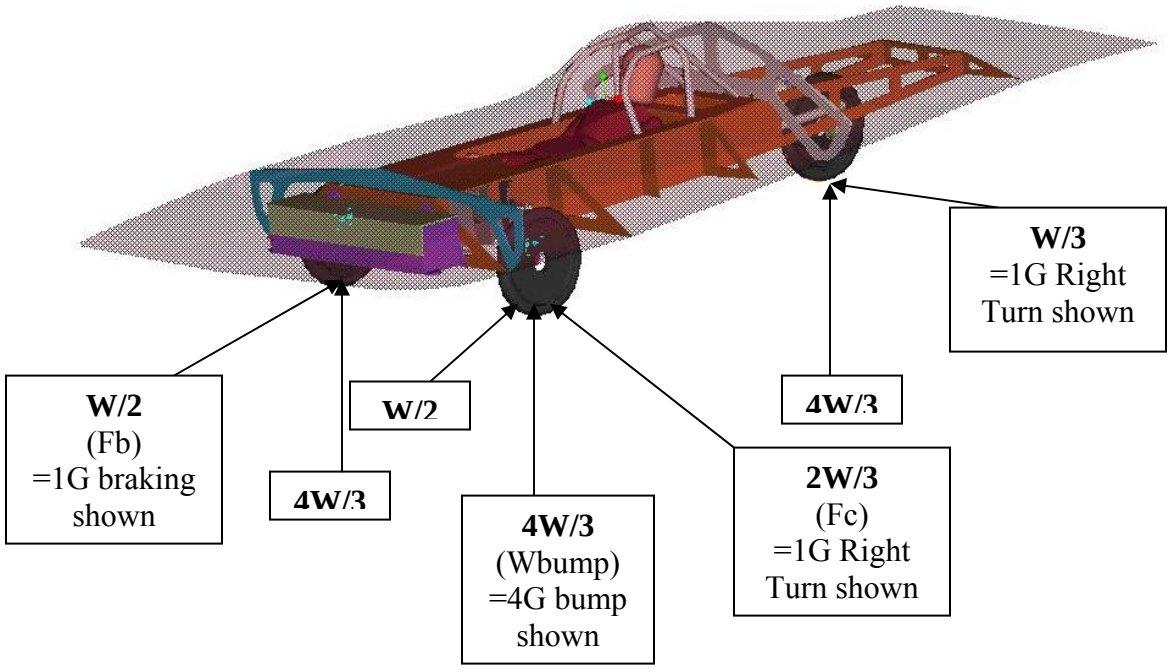


**Figure 26: Assumed Loading Conditions**